



Fabrication of β -Ni(OH)₂ Particles by Alkaline Etching Layered Double Hydroxides Precursor for Supercapacitor

Lumei Chen, Xiaotong Yang, Ye Tian, Yiping Wang, Xuhui Zhao, Xiaodong Lei and Fazhi Zhang*

State Key Laboratory of Chemical Resource Engineering Beijing University of Chemical Technology, Beijing, China

OPEN ACCESS

Edited by:

Shilin Zhang,
University of Adelaide, Australia

Reviewed by:

Yan Lu,
Shandong University, China
Li Li,
Shanghai University, China
Ye Liu,
Humboldt University of Berlin,
Germany

*Correspondence:

Fazhi Zhang
zhangfz@mail.buct.edu.cn

Specialty section:

This article was submitted to
Electrochemical Energy Conversion
and Storage,
a section of the journal
Frontiers in Energy Research

Received: 07 November 2021

Accepted: 22 November 2021

Published: 03 January 2022

Citation:

Chen L, Yang X, Tian Y, Wang Y,
Zhao X, Lei X and Zhang F (2022)
Fabrication of β -Ni(OH)₂ Particles by
Alkaline Etching Layered Double
Hydroxides Precursor
for Supercapacitor.
Front. Energy Res. 9:810568.
doi: 10.3389/fenrg.2021.810568

We report the facile preparation of β -Ni(OH)₂ particles by etching a NiAl-**layered double hydroxides** (NiAl-LDHs) precursor with KOH solution. The amphoteric Al³⁺ ions in LDHs crystal were selectively dissolved out by KOH solution and LDHs crystals were proposed to be *in situ* topologically transformed to form β -Ni(OH)₂. Alkaline concentration has a great influence on the structure, morphology, specific surface area, and porous structure of the resulting samples. Compared to LDHs precursor and β -Ni(OH)₂ prepared by a precipitation reaction, the sample etched in 10 M KOH solution has enhanced specific capacitance (829 F/g at 1 A/g), high rate capability (capacitance retention 57.3% with current density 8 A/g), and good charge/discharge stability. We suggested that the high accessible specific surface area and appropriate porous structure, which is conducive to full contact between active material and electrolyte, can improve the utilization rate of the active material to increase the rate capacity of the 10 M KOH-etched sample.

Keywords: β -Ni(OH)₂, LDHs, alkaline etching, topological transformation, pseudocapacitor

INTRODUCTION

In the 21st century, environmental pollution and energy problems have become the focus of attention. Coal, oil, and other energy sources that cause pollution irrefutably need to have their usage reduced. It is, therefore, urgent to look for clean, non-polluting, sustainable energy technologies, and in recent years electrochemical energy storage systems, especially the popular lithium-ion batteries, have been used as fast and efficient energy storage/release devices (Zhang et al., 2021).

In the battery, the number of transported ions is large, which is conducive to the improvement of performance. Some researchers have studied the storage mechanism of potassium ion batteries and other potassium-based storage systems that may be applied (Zhang et al., 2020; Zhou et al., 2020). Moreover, it has been found that the supercapacitor has some excellent characteristics: the charging and discharging rate is fast, it possesses a high energy density, has good cycle stability, and it is suitable for energy storage devices—it has great potential (Simon and Gogotsi, 2008; Zhang et al., 2017; Šekularac et al., 2017).

There are two types of supercapacitors. Electric double-layer capacitors, that store energy by absorbing charge on the electrode surface, have the advantages of good power density and stability but have the disadvantage of low specific capacitance. The second type is pseudocapacitors that store energy through the redox reaction of active electrode materials, the advantages are high capacitance and energy density, but the disadvantages are very poor stability (Yu et al., 2015). Among the

pseudocapacitive materials of transition metal hydroxides, Ni(OH)₂ has a clear redox transition, and its theoretical ratio is higher than its capacitance, while the material cost is low. Therefore, Ni(OH)₂ is recognized by researchers as an excellent material for supercapacitors (Wang et al., 2010; Yu et al., 2015). There are two kinds of Ni(OH)₂, α -Ni(OH)₂ and β -Ni(OH)₂, their crystal forms being different. The former is composed of stacked nickel hydroxide lamellar plates, inserted anions, and water molecules, while the latter is similar to hexagonal magnesite structure, without anionic and water molecular intercalation. In a strong alkaline environment, β -Ni(OH)₂ has good reversibility and structural stability (Oliva et al., 1982; Bernard et al., 1996; Neiva et al., 2016). Therefore, it is believed that it may show excellent electrochemical performance, but the results of the tests show that β -Ni(OH)₂ based electrodes have poor rate performance and stability, which is not conducive to its practical application (Wang et al., 2010). For improving the rate of performance and stability of β -Ni(OH)₂, many researchers have tried to improve the specific surface area, which is beneficial for the electrolyte solution to contact the electrode material more effectively. Zhou et al. prepared β -Ni(OH)₂ by adjusting anions in nickel salt. The results show that the materials prepared with NiSO₄ are the best, its specific surface area reached 94.8 m²/g, and 1,025.3 F/g at 1 A/g (Zhou et al., 2014). Another example introduced the synthesis of nanorod by a surfactant-free water precipitation method with surface area 91 m²/g, showing 1,150 F/g at 1 mV/s, after 5,000 cycles, the capacitance retention is more than 99% (Lakshmi et al., 2014). Moreover, controlling the assembly of crystal sheets to generate various assemblies is also a great method. Several assembly forms are possible: snow spheres (Tian et al., 2013), coin-like nanoplates (Li et al., 2011), flower-like nanostructures (Tang et al., 2014), pompon-like microspheres with hollow interiors (Wang et al., 2013), microspheres with cracks (Yan et al., 2013), and microspheres composed of nanowires (Luo et al., 2011). According to various literature, several fabrication strategies, such as gas-liquid co-deposition method (Tian et al., 2013), coordination homogeneous precipitation method (Li et al., 2011), hydrothermal synthesis (Wang et al., 2013; Yan et al., 2013; Tang et al., 2014; Boychuk et al., 2019), electrodeposition method (Tizfahm et al., 2014), chemical precipitation (Xiao-yan and Jian-Cheng, 2007), solvothermal (Kalam et al., 2013), and sonochemical (Vidotti et al., 2006), have been used to prepare the β -Ni(OH)₂ assembly materials with high pseudocapacitive characteristics. In addition, the introduction of divalent and trivalent cations, such as Co²⁺ (Wang et al., 2019a), Zn²⁺ (Li et al., 2013), Co²⁺ and Zn²⁺ (Park et al., 2006), Al³⁺ (Huang et al., 2013), and La³⁺ (Shao et al., 2009; Chakrabarty and Chakraborty, 2019) into the β -Ni(OH)₂ lattice is a good strategy for enhancing discharge capacity and utilization of active substances, which may be related to stable layered structure and the increase of anion transfer rate. How to fabricate facilely a new β -Ni(OH)₂-based electrode material with high accessible surface area to obtain excellent performance, however, is still worth exploring.

LDHs are a kind of anionic hydroxide-like functional material (Yu et al., 2017; Wang et al., 2019b). LDHs structure is similar to the β -Ni(OH)₂, and the main laminar plates are

formed by the edges of MO₆ octahedrons. Because of the crystal structure characteristics of LDHs materials, the structure and composition can be designed by adjusting the main laminates and guest molecules, so as to greatly improve the functional combination performance, and they can be applied to many fields of the national economy (Li et al., 2014; Kang et al., 2017; Mishra et al., 2018). Also, Ni-containing LDHs materials have been reported as energy storage materials (Yin and Tang, 2016; Gao et al., 2020). However, LDHs materials have a strong superposition tendency, resulting in poor conductivity and slow ion transfer speed, which seriously limits their application in supercapacitors (Zhao et al., 2017).

Herein, NiAl-LDHs were adopted as a precursor for fabrication of β -Ni(OH)₂ particles with enhanced specific surface area through KOH alkaline etching. The amphoteric Al³⁺ ions in the LDHs crystal were selectively dissolved out by the KOH solution. The alkaline concentration greatly affects the structure, morphology, and specific surface area of the resulting samples. On the basis of sample characterization results, we suggested an *in situ* topological transformation mechanism of β -Ni(OH)₂ from NiAl-LDHs precursor by alkaline etching. Finally, the electrochemical performance was tested, exhibiting excellent pseudocapacitor performance. We proposed that the high accessible surface area and appropriate porous structure, which can make the electrode material contact with the electrolyte solution more fully, can improve the utilization rate of the active material to increase its rate capacity. The preparation method we presented is simple and easy and has a prominent capacitive performance. It has certain application prospects.

EXPERIMENTAL

Materials Preparation

Preparation of NiAl-LDHs Precursor

NiAl-LDHs precursor sample was synthesized by hydrothermal method. Firstly, 0.818 g Ni(NO₃)₂·6H₂O, 0.352 g Al(NO₃)₃·9H₂O, and 0.496 g urea were mixed in a beaker, then add 50 ml deionized water, and the total metal ion content was 1.875 mmol. Afterward, it was crystallized at 120°C for 24 h. Finally, the samples were cooled to room temperature, centrifuged and washed to pH 7.0, and vacuum-dried overnight at 50°C.

The β -Ni(OH)₂ comparison sample was synthesized by precipitation reaction. A measure of 3.837 g Ni(NO₃)₂·6H₂O and 2.191 g NaOH, were dissolved in 20 and 50 ml deionized water, respectively. Then, the Ni(NO₃)₂·6H₂O solution was dropped into the NaOH solution by single drop method under agitation conditions, and the pH was kept at 10.0. Afterward, it was crystallized at 120°C for 6 h. Finally, the reaction was centrifuged and washed to pH 7.0 and dried at 70°C overnight.

Preparation of Alkaline-Etched Samples

NiAl-LDHs were immersed in 5, 10, and 15 M KOH solution for stirring 3 h continuously at 60°C. After that, they were centrifuged and washed to pH 7.0. The washed samples were dried.

Sample Characterization

The X-ray diffraction (XRD) pattern was recorded on a Shimadzu XRD-6000 diffractometer using Cu K α radiation ($\lambda = 1.5406 \text{ \AA}$), $10^\circ \text{ min}^{-1}$ at $3\text{--}80^\circ$. A scanning electron microscope (SEM) was carried out on a Zeiss Supra 55. Fourier transform infrared spectroscopy (FT-IR) was tested on Bruker Vector-22 and the range is $400\text{--}4,000 \text{ cm}^{-1}$. Elemental analysis was tested on Shimadzu IPCPS-7500. High-resolution transmission electron microscopy (HRTEM) was conducted on a JEOL JEM-2100F instrument, point resolution is 0.19 nm . X-ray photoelectron spectroscopy (XPS) was measured by using an ESCALAB250 X-ray photoelectron spectrometer equipped with monochromatized Mg K α X-ray radiation ($1,253.6 \text{ eV}$ photons). BET and BJH methods were used to measure specific surface area and analyze pore volume and size, using a Quantachrome Autosorb-1C-VP Analyzer.

Electrochemical Measurement

Electrochemical tests were carried out on an electrochemical workstation (CHI 618E, Shanghai ChenHua Corporation, China), in a 2 M KOH solution. Active material: acetylene black: polyvinylidene fluoride at $8:1:1$, then dissolved with an appropriate amount of ethanol and dropped onto $1 \text{ cm} \times 1 \text{ cm}$ nickel foam. Dried at 60°C for 30 min and pressed by roller press with proper pressure. The sample loaded onto each working electrode was about 2 mg . The cyclic voltammetry (CVs) curves were recorded within $0.0\text{--}0.6 \text{ V}$ at 5 mV/s . Galvanostatic charge-discharge (GCD) measurements were tested at $0.0\text{--}0.45 \text{ V}$ from 1 to 8 A/g . Electrochemical impedance spectroscopy (EIS) measurements were performed under an AC voltage of 5 mV and the frequency was $0.01\text{--}100 \text{ kHz}$. Specific capacitance was calculated by using the equation below, where I represents the discharge current; t represents time; ΔV represents the voltage drop upon discharging; m represents the mass of the sample.

$$C = It/\Delta Vm$$

RESULTS AND DISCUSSION

NiAl-LDHs precursor was synthesized by a hydrothermal method. The XRD pattern demonstrates that the precursor sample has the characteristic feature of layered material (Figure 1). The (003) peak appears at 11.53° , which is consistent with JCPDS No.15-0087, indicating that carbonate anions are intercalated in the LDHs gallery (Li et al., 2019). SEM image of LDHs precursor shows the irregular morphology of nanosheets with a length of about $200\text{--}400 \text{ nm}$ and thickness about 20 nm (Figure 2A). Subsequently, the LDHs precursor sample was immersed in different concentrations of KOH solution for dealumination. The characteristic XRD peaks of LDHs in the 5 M KOH alkaline-etched sample are slightly enhanced (Figure 1), demonstrating that after etching, the crystallinity of the crystal is improved, which may be due to the change of coordination environment of metal elements in the

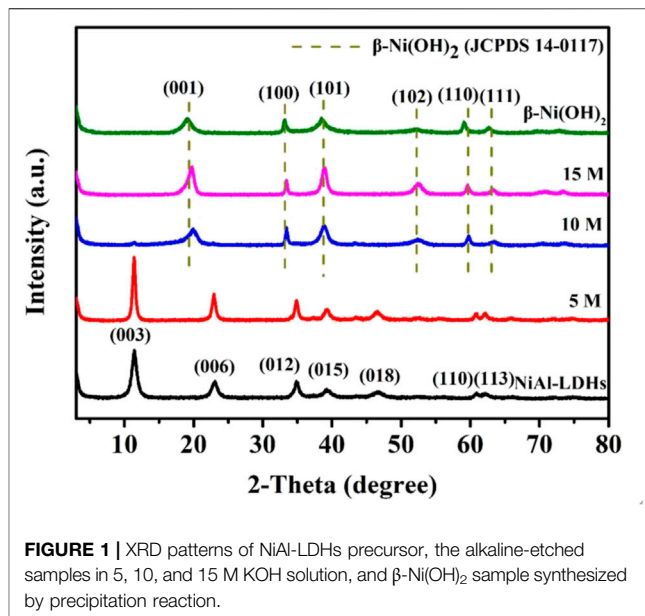


FIGURE 1 | XRD patterns of NiAl-LDHs precursor, the alkaline-etched samples in 5 , 10 , and 15 M KOH solution, and β -Ni(OH)₂ sample synthesized by precipitation reaction.

lamella. Partial dealumination by 5 M KOH alkaline may form α -Ni(OH)₂/NiAl-LDHs compound. The α -Ni(OH)₂ phase has the same crystal structure and characteristic XRD peaks as LDHs (Gong et al., 2013). The α -Ni(OH)₂ can also be proved by the fact that there are two pairs of redox peaks in the CV curve and two pairs of platforms in the GCD curve in the subsequent electrochemical performance test (Figure 7A). SEM image of the 5 M alkaline-etched sample shows that the morphology of the nanosheet becomes more regular, with a length of about $150\text{--}200 \text{ nm}$ and thickness about 40 nm (Figure 2B). After 10 M alkaline treatment, the characteristic XRD reflections of LDHs vanish and several new peaks appear, indicating that the collapse and crystal transformation of LDHs laminates occur simultaneously (Figure 1). The newly main diffraction peaks at 19.9° , 33.4° , 38.8° , 52.45° , 59.8° , and 63.4° 2θ could be indexed to the (001), (100), (101), (102), (110), and (111) facets of β -Ni(OH)₂, these peak positions are consistent with the standard cards (JCPDS No.14-0117) (Wang et al., 2012). Further investigation by SEM image shows that the crystal sheets of the 10 M alkaline-etched sample become thinner and larger compared to those of LDHs precursor, the length is about $400\text{--}500 \text{ nm}$ and thickness about 10 nm (Figures 2C,D). It is known that the positive charge of the LDHs laminates and the negative ions between layers keep the charge in balance; while there is no intercalation of anions and water molecules in β -Ni(OH)₂. The decrease in thickness of the sheets because of the dehydration and deionization between the LDHs layers after the strong alkaline treatment, which can be identified by the following FT-IR result (Figure 3). XRD pattern of the 15 M alkaline-etched sample is similar to that of the 10 M alkaline-etched one (Figure 1). However, the nanosheets are broken and the particle thickness is increased in the 15 M alkaline solution (Figure 2E), which may be due to the structural cracking and

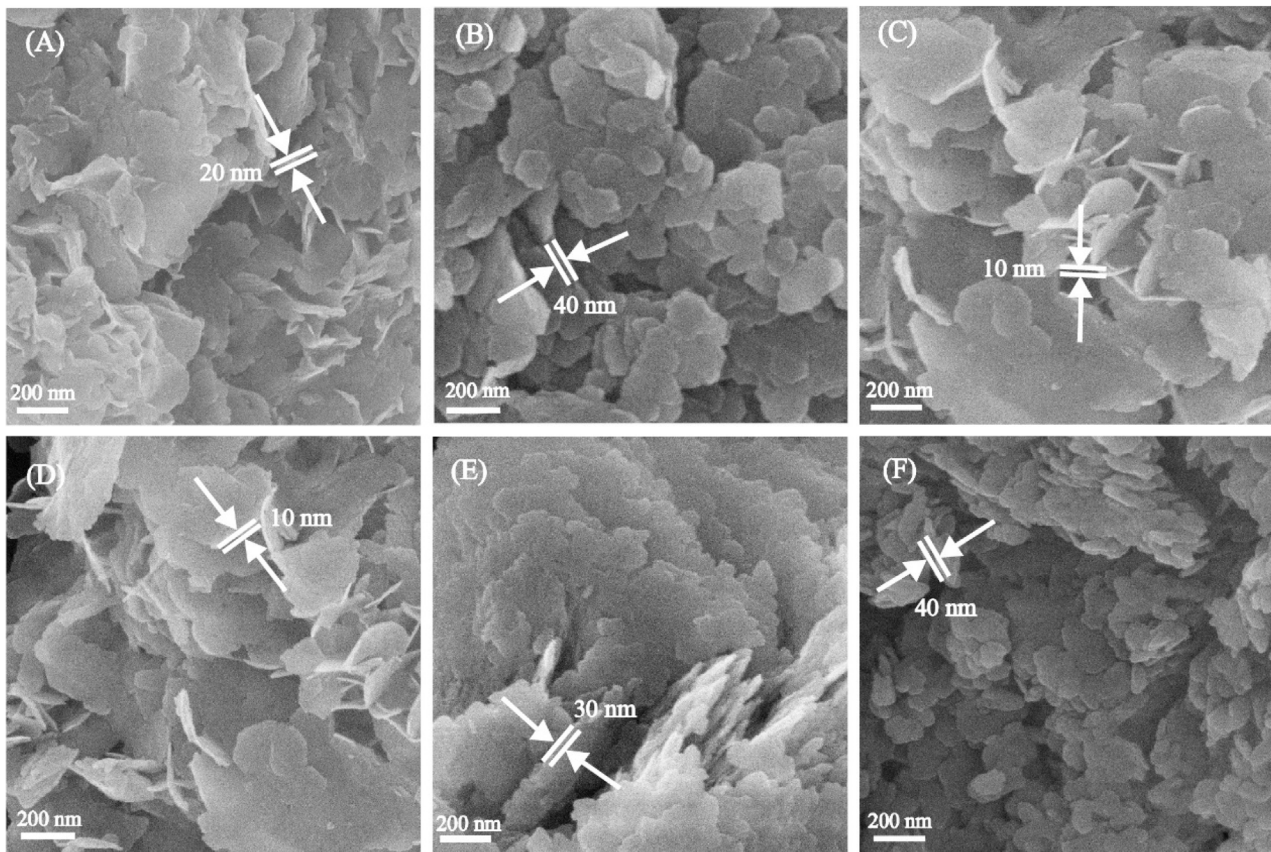


FIGURE 2 | SEM images of NiAl-LDHs precursor (A), the alkaline-etched samples in 5 (B), 10 (C,D), and 15 (E) M KOH solution, and β -Ni(OH)₂ sample prepared by precipitation reaction (F).

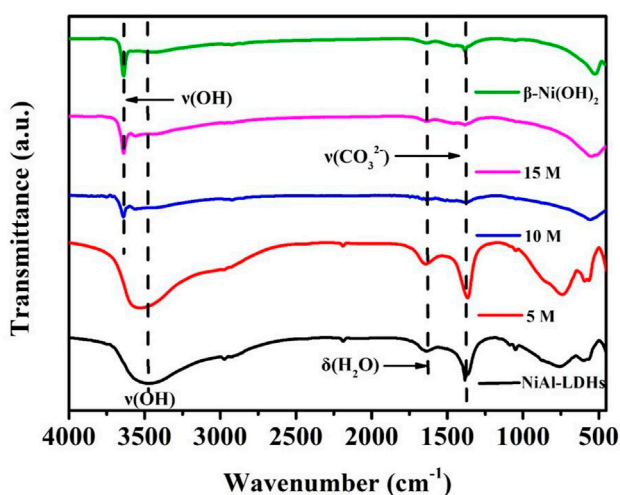


FIGURE 3 | FT-IR spectra of NiAl-LDHs precursor, the alkaline-etched samples in 5, 10, and 15 M KOH solution, and β -Ni(OH)₂ sample prepared by precipitation reaction.

continuous accumulation of nanosheets. The length and thickness of β -Ni(OH)₂ contrast sample is about 100 and 40 nm respectively (Figure 2F).

The identities of interlayer anions and water molecules of NiAl-LDHs precursor, as well as the alkaline-etched samples in 5, 10, and 15 M KOH solution and β -Ni(OH)₂ sample, were characterized by FT-IR spectra in the range of 400–4,000 cm⁻¹ (Figure 3). For NiAl-LDHs precursor, the intense IR band at 3,475 cm⁻¹ is characteristic for the ν (OH) stretching vibration of the LDHs laminate OH group and interlayer water molecules. The other peaks observed at 1,640 and 1,360 cm⁻¹ are assigned to δ (H₂O) and ν (CO₃²⁻) bending vibration, respectively (Hunter et al., 2016). The 5 M alkaline-etched sample shows a similar spectrum to that of NiAl-LDHs precursor. For the 10 and 15 M alkaline-etched samples, the 1,640 and 1,360 cm⁻¹ peaks vanish, demonstrating the complete dehydration and deionization between the LDHs layers. Moreover, the peak at 3,640 cm⁻¹ represents the stretching vibration of ν (OH), the peak positions of the two samples are consistent with that of the synthesized β -Ni(OH)₂ sample, confirming the formation of β -Ni(OH)₂ after 10 and 15 M alkaline treatment (Aghazadeh et al., 2011).

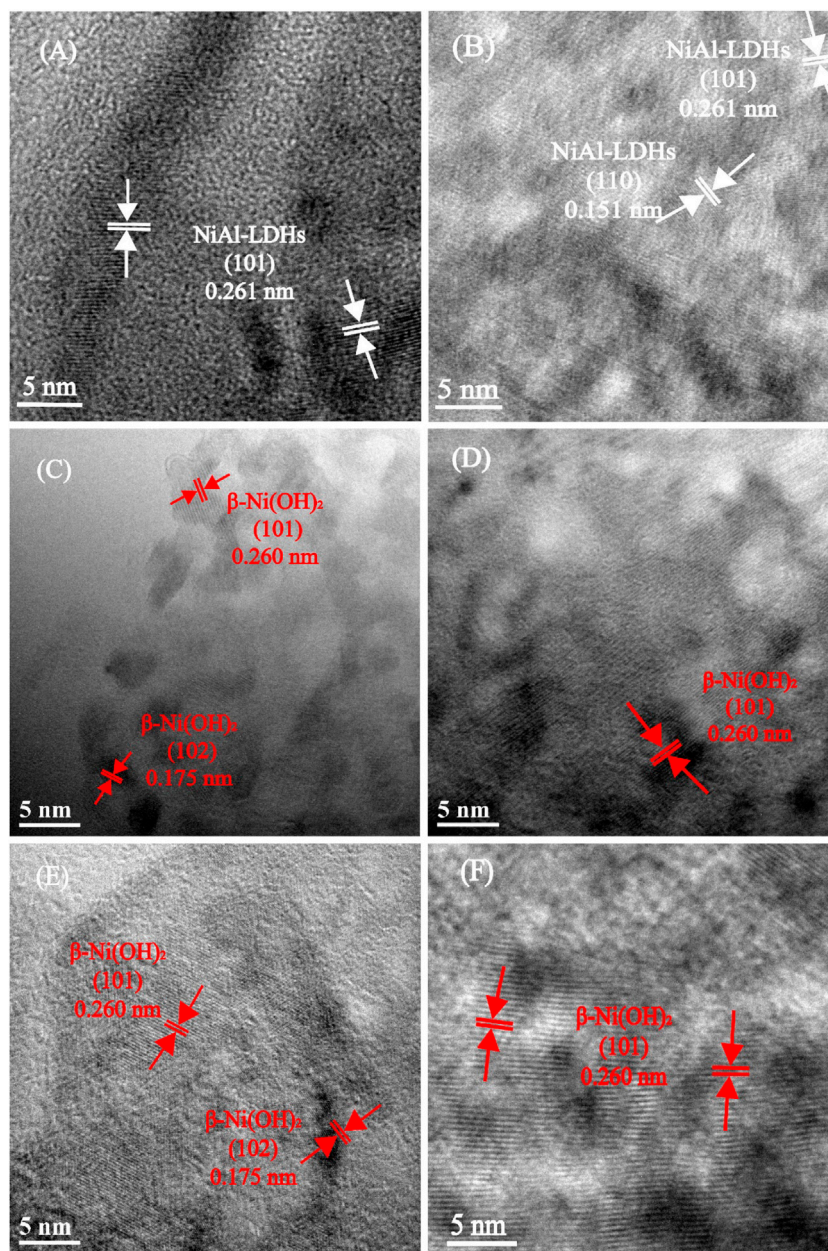
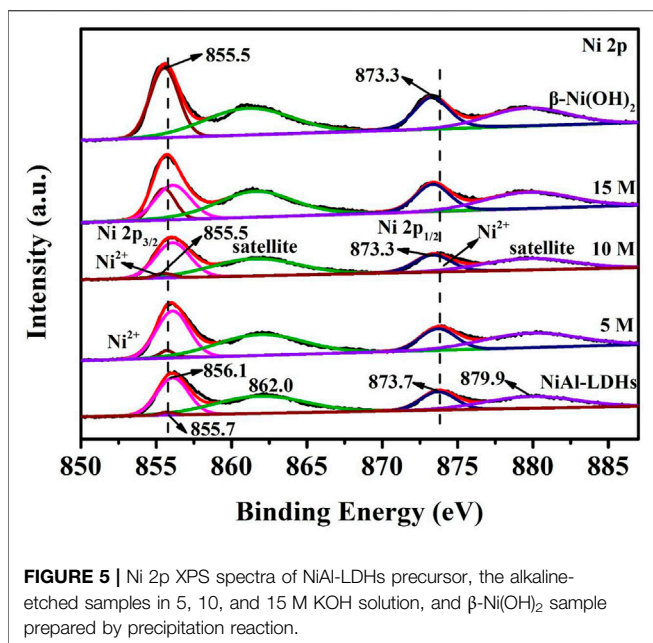


FIGURE 4 | HRTEM images of NiAl-LDHs precursor **(A)**, the alkaline-etched samples in 5 **(B)**, 10 **(C,D)**, and 15 **(E)** M KOH solution, and β -Ni(OH)₂ sample prepared by precipitation reaction **(F)**.

ICP techniques were used to confirm the change of composition during alkali etching. ICP analysis shows that the Ni:Al molar ratio of LDHs precursor is about 3:1, which is similar to that in the starting synthetic solution. After alkali treatment in 5, 10, and 15 M KOH solution, the Al contents are gradually reduced from 24.1% in LDHs precursor to 22.8% in 5 M alkaline-etched sample, 10.3% in 10 M alkaline-etched sample, and finally to 8.5% in 15 M alkaline-etched sample, which demonstrates that the Al³⁺ in LDHs crystal is successfully removed.

The HRTEM technique can analyze the structure and phase distribution of the resulting samples (**Figure 4**). For NiAl-LDHs

precursor, the lattice spacings of 0.261 nm match well with the (101) crystal facet of LDHs (**Figure 4A**). After 5 M alkaline treatment, the crystal phase becomes ordered and the crystal region expands, indicating that the lattice rearrangement occurs. The measurements of 0.261 and 0.151 nm match well with the (101) and (110) crystal facets of LDHs, respectively (**Figure 4B**). For the 10 M alkaline-etched sample, the lattice fringes of adjacent stripes are measured to be 0.260 and 0.175 nm which can be allotted to the (101) and (102) crystal facets of β -Ni(OH)₂, respectively (Li et al., 2010) (**Figures 4C,D**). Moreover, the lattice spacing of 0.260 nm in the 15 M KOH-etched sample (**Figure 4E**)



and the synthesized β -Ni(OH)₂ (Figure 4F) also correspond to the (101) crystal plane.

The surface composition and metal chemical state of the samples were studied by XPS technique (Figure 5). The characterization range of Ni 2p XPS peak is 850.0–887.0 eV. For the LDHs precursor sample, the Ni 2p spectrum shows five deconvoluted peaks at 855.7, 856.1, 862.0, 873.7, and 879.9 eV. Among these, the peaks at 855.7 and 856.1 eV represent Ni²⁺ 2p_{3/2} and the peak at 873.7 eV represents Ni²⁺ 2p_{1/2}. Signals locate at 862.0 and 879.9 eV are the satellite peaks of Ni²⁺ 2p_{3/2} and Ni²⁺ 2p_{1/2}, respectively (Wu et al., 2018; Ye et al., 2018; Wang et al., 2021a). The 5 M alkaline-etched sample has five binding energies similar to those of the LDHs precursor. After alkaline treatment in 10 M KOH solution, the peaks of Ni²⁺ 2p_{3/2} and Ni²⁺ 2p_{1/2} move to 855.5 and 873.3 eV, which are characteristic of β -Ni(OH)₂ (Huang et al., 2017). XPS spectrum of the 15 M alkaline-etched sample is similar to that of the 10 M alkaline-etched one, and the peaks at 855.5 and 873.3 eV also correspond to the β -Ni(OH)₂ sample.

N₂-adsorption/desorption measurement was carried out for investigating the surface area and porosity property of the five resulting samples (Figure 6). In all the cases, when P/P₀ is high, the isotherms exhibit hysteresis due to capillary condensation (Zhai et al., 2019). BET specific surface areas of NiAl-LDHs precursor, the alkaline-etched samples in 5, 10, and 15 M KOH solution, and β -Ni(OH)₂ sample prepared by precipitation reaction are measured to be 64, 56, 79, 60, and 37 m²/g, respectively, with their pore diameter mostly distributes at 11.6, 24.8, 2.4, 22.6 and 23.6 nm, respectively. It is reported that the performance of supercapacitor is better when the aperture is 2–5 nm (Shao et al., 2012). These properties are the result of the interstitial space among the nanosheets (Mao

et al., 2020). As the crystallinity of the sample etched in 5 M KOH solution increased slightly, the nanosheets became more regular, resulting in a smaller specific surface area than the precursor samples. For the 10 M alkaline-etched sample, the particle morphology may change through an Ostwald ripening process (Hall et al., 2015). The relatively small stacked particles on the surface of large LDHs particles tend to dissolve in the solution, and then the dissolved substances are sequentially deposited on the edge of the larger LDHs layer (Chen et al., 2018), leading to thinner and larger nanosheets (Figures 2C,D). At a higher 15 M alkaline solution, the nanosheets begin to break and stack, and the specific surface area decreases.

Based on the above characterization results, we propose a possible transformation mechanism of β -Ni(OH)₂ from NiAl-LDHs precursor by alkaline etching. Previous studies have shown that a series of high-performance layered mixed metal oxides can be prepared by using the topological transformation of LDHs precursors under high-temperature calcination (Liu et al., 2018; Xu and Wei, 2018). β -Ni(OH)₂ has a hexagonal structure similar to magnesite. Therefore, we believe that the transformation of NiAl-LDHs to β -Ni(OH)₂ under alkaline etching is a topological transformation process. In the early stage of alkaline etching, a small number of unstable aluminum atoms are selectively removed, resulting in the formation of lattice vacancies. Due to the leaching of partial aluminum atoms from LDHs laminate, the surface energy increases with the decrease of the coordination number of surface atoms. The remaining metal atoms migrate and rearrange the lattice to form a relatively stable lamellar structure, producing α -Ni(OH)₂/NiAl-LDHs compound (Chen et al., 2021). In addition, the removal of Al leads to the decrease of positive charge in the main layer, which causes the diffusion of charge-balancing anions (CO₃²⁻) from the LDHs gallery. α -Ni(OH)₂ is extremely unstable in a concentrated alkaline environment (Jian et al., 2016). When the alkali concentration reaches 10 M, the interlamellar water molecules and CO₃²⁻ are almost completely removed (Figure 3), and XRD result shows that it is converted to the more stable β -Ni(OH)₂, at this point, the topological transformation process is completed.

Electrochemistry properties of the resulting samples, including CVs, GCD, EIS, and cycle stability were evaluated. Figure 7A shows CVs of different electrode materials at 5 mV/s. CVs curves of NiAl-LDHs precursor, the alkaline-etched samples in 10, 15 M KOH solution, and β -Ni(OH)₂ prepared by precipitation reaction consist of a pair of Ni²⁺/Ni³⁺ redox peaks that convert each other (equation 1).



Interestingly, however, another pair of redox peaks appeared in the 5 M alkaline-etched sample. In addition to the above redox reaction Ni(OH)₂ ↔ NiOOH, the second oxidation/reduction potential peaks are located at 0.45 and 0.3 V, which is attributed to the reversible redox α -Ni(OH)₂ ↔ γ -NiOOH (Huang et al., 2013). Moreover, Figure 7A shows that the average area of the CV curve of the 10 M alkaline-etched sample is much larger than that of other samples. Figure 7B displays the GCD of different samples within 0–0.45 V. The curve is nonlinear, which proves its

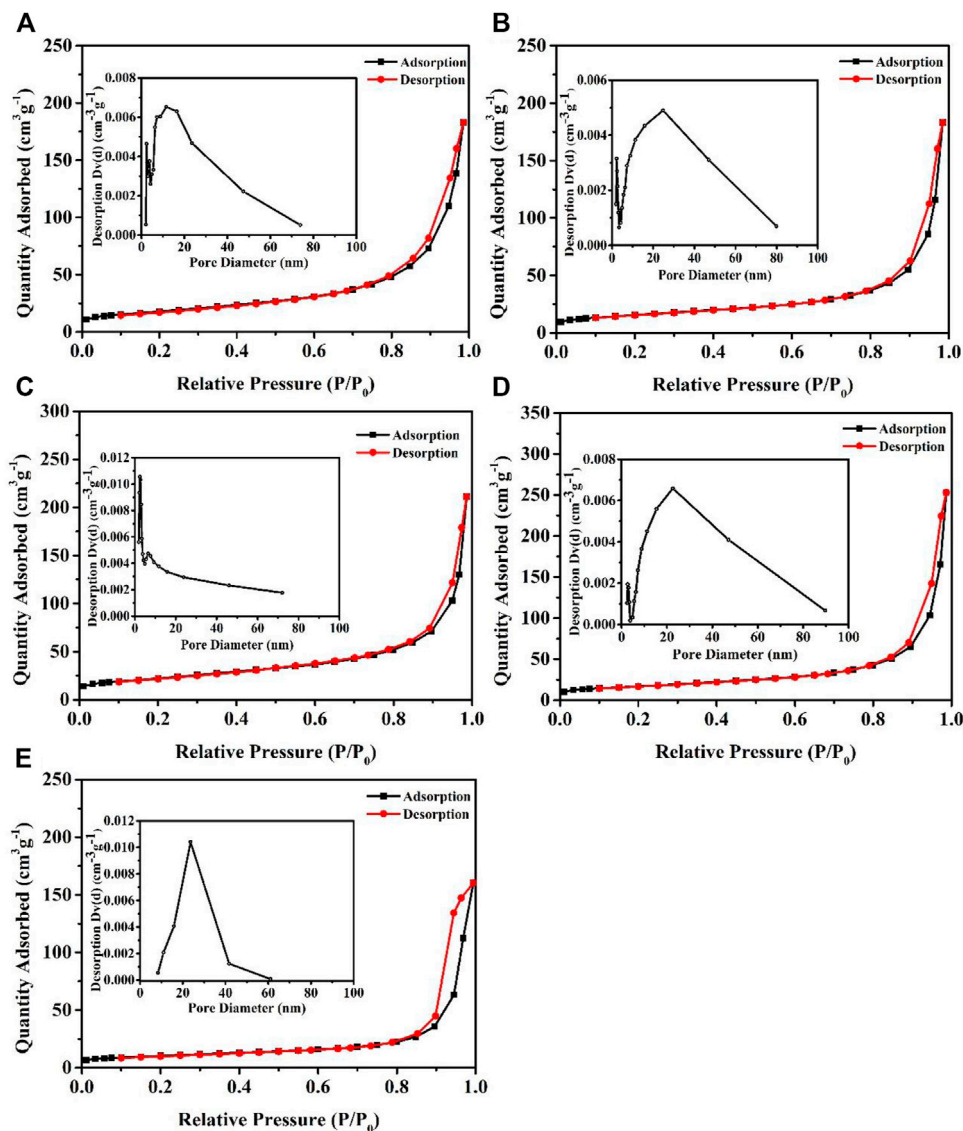


FIGURE 6 | N_2 -adsorption isotherms and pore size distribution (inset) of NiAl-LDHs precursor (A), the alkaline-etched samples in 5 (B), 10 (C), and 15 (D) M KOH solution, and β -Ni(OH)₂ sample prepared by precipitation reaction (E).

pseudocapacitance property (Jiang et al., 2011). The corresponding measured specific capacitance is 552, 319, 829, 452, and 463 F/g at 1 A/g for the NiAl-LDHs precursor, the alkaline-etched samples in 5, 10, 15 M KOH solution, and β -Ni(OH)₂, respectively, which further confirms that the 10 M alkaline-etched sample has the highest specific capacitance. The high specific surface area (79 m²/g) and an appropriate porous structure (2.4 nm) of 10 M alkaline-etched sample, which can make the contact between the solution and the substance more sufficient, at the same time, the ion migration is more rapid, and obtain good specific capacitance performance.

The specific capacitances of the five samples at different current densities are shown in Figure 7C. At 8 A/g, the retention rate is 57.3% (from 829 to 475 F/g) for the 10 M alkaline-etched sample, whereas the NiAl-LDHs precursor

31.3%, the 5 M sample 17.2%, the 15 M sample 41.2%, and the β -Ni(OH)₂ sample prepared by precipitation reaction 62.6%. A large specific surface area and suitable mesoporous structure make the electrolyte easy to transport, which is conducive to the improvement of specific capacitance and rate performance (Shen et al., 2018); dealumination by alkaline etching is also conducive to the improvement of rate performance (Wang et al., 2021b). The 10 M alkaline-etched sample is mainly due to the combination of high specific surface area, suitable pore size, and dealumination to improve performance.

We also performed EIS measurements to investigate their performance. Figures 7D,E shows the EIS for the five samples (Figure 7E is a larger version of the Nyquist plots of Figure 7D). The semicircle diameter of EIS refers to the electron transfer resistance of Ni²⁺/Ni³⁺ during the redox process (Ret) (Di Fabio

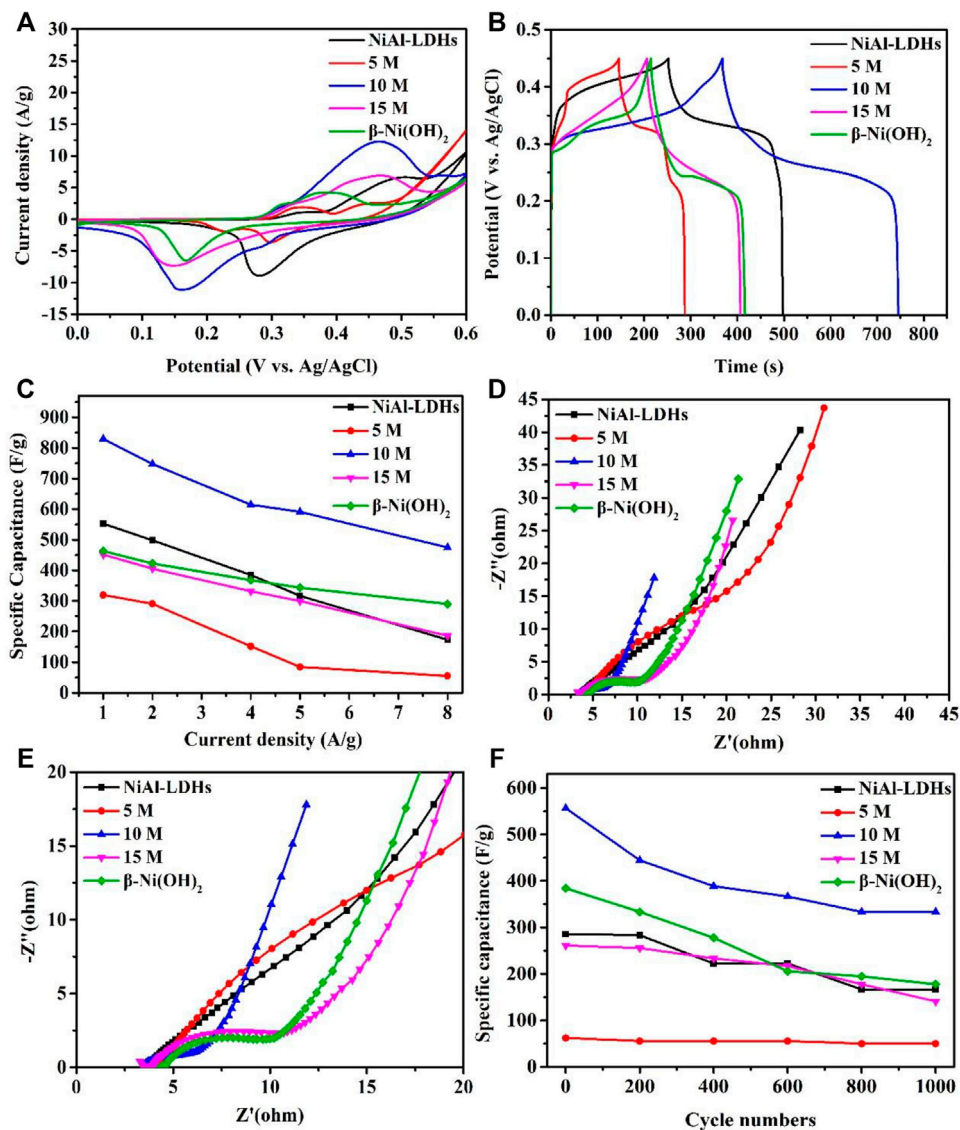


FIGURE 7 | Supercapacitive performance of NiAl-LDHs precursor, the alkaline-etched samples in 5, 10, and 15 M KOH solution, and β -Ni(OH)₂ sample prepared by precipitation reaction. **(A)** CVs curves at 5 mV/s; **(B)** GCD curves at 1 A/g within 0–0.45 V; **(C)** Specific capacitance at different current density; **(D)** Nyquist plots of EIS, showing the imaginary part versus the real part of impedance; **(E)** a larger version of Nyquist plots of (d); **(F)** cycle performance measured at 5 A/g for 1,000 cycles.

et al., 2001; Zang et al., 2008). We can see that 10 M alkaline-etched sample < β -Ni(OH)₂ sample < 15 M alkaline-etched sample < 5 M alkaline-etched sample < NiAl-LDHs precursor, which clearly demonstrates that the 10 M alkaline-etched sample has the lowest resistance, so electrons transfer faster. It is found that the reversible absorption and release of OH⁻ in solution and the transfer of electrons on the collector occur during the redox process of Ni-based hydroxide as the electrode material of supercapacitor (Kötz and Carlen, 2000; Liu et al., 2011). The lower resistance of the 10 M alkaline-etched sample, may be due to the higher specific surface area which facilitates the effective exposure of active sites, and may also be related to the modification of the Ni coordination environment by Al

etching (Liu et al., 2017). However, the specific surface areas of 5 and 15 M alkaline-etched samples decrease due to different degrees of stacking, resulting in a larger pore size distribution than the most suitable pore size of a supercapacitor, and a larger resistance, which is not conducive to the performance of a supercapacitor. Moreover, the 5 M alkaline-etched sample did not form β -Ni(OH)₂, so the electrochemistry performance of this sample is worse than that of the 15 M alkaline-etched sample. On the other hand, **Figure 7F** shows the stability of 1,000 cycles of each sample at 5 A/g. The 10 M alkaline-etched sample can retain about 60% (from 557 to 333 F/g), and also shows the largest specific capacitance after 1,000 cycles.

CONCLUSIONS

We report a facile method for the fabrication of β -Ni(OH)₂ particles by KOH alkaline etching NiAl-LDHs precursor with improved supercapacitor performance. The amphoteric Al³⁺ ions in LDHs crystal were selectively dissolved out by the KOH solution and the alkaline concentration affect greatly the structure, morphology, specific surface area, and porous structure of the resulting samples. On the basis of sample characterization results, we propose an *in situ* topological transformation mechanism of β -Ni(OH)₂ from NiAl-LDHs precursor by alkaline etching. Compared to NiAl-LDHs precursor and β -Ni(OH)₂ sample, the obtained β -Ni(OH)₂ sample etching in 10 M KOH alkaline has enhanced specific capacitance, high rate capability, and good charge/discharge stability. We propose that high accessible specific surface area and appropriate porous structure are conducive to the full contact between active materials and electrolytes, improve the utilization of active materials, shorten the migration path of ions, improve the rated capacity of alkaline-etched samples, and have good electrochemical performance. Our findings

show an example for the effective fabrication of β -Ni(OH)₂-based electrode material.

DATA AVAILABILITY STATEMENT

The original contributions presented in the study are included in the article/Supplementary Material, further inquiries can be directed to the corresponding author.

AUTHOR CONTRIBUTIONS

LM did the experiments, processed the data, and wrote the paper. FZ designed the experiments and revised the paper. XT and other teachers provided very valuable suggestions in the process.

FUNDING

This work was supported by the National Natural Science Foundation of China (No. 21376019, 21676013).

REFERENCES

- Aghazadeh, M., Golikand, A. N., and Ghaemi, M. (2011). Synthesis, Characterization, and Electrochemical Properties of Ultrafine β -Ni(OH)₂ Nanoparticles. *Int. J. Hydrogen Energ.* 36 (14), 8674–8679. doi:10.1016/j.ijhydene.2011.03.144
- Bernard, M. C., Bernard, P., Keddad, M., Senyari, S., and Takenouti, H. (1996). Characterisation of New Nickel Hydroxides during the Transformation of a Ni(OH)₂ to β Ni(OH)₂ by Ageing. *Electrochimica Acta* 41 (1), 91–93. doi:10.1016/0013-4686(95)00282-j
- Boychuk, V., Kotsyubynsky, V., Rachiy, B., Bandura, K., Hrubciak, A., and Fedorchenko, S. (2019). β -Ni(OH)₂/Reduced Graphene Oxide Composite as Electrode for Supercapacitors. *Mater. Today Proc.* 6, 106–115. doi:10.1016/j.matpr.2018.10.082
- Chakraborty, N., and Chakraborty, A. K. (2019). Controlling the Electrochemical Performance of β -Ni(OH)₂/carbon Nanotube Hybrid Electrodes for Supercapacitor Applications by La Doping: A Systematic Investigation. *Electrochimica Acta* 297, 173–187. doi:10.1016/j.electacta.2018.11.174
- Chen, B., Zhang, Z., Kim, S., Lee, S., Lee, J., Kim, W., et al. (2018). Ostwald Ripening Driven Exfoliation to Ultrathin Layered Double Hydroxides Nanosheets for Enhanced Oxygen Evolution Reaction. *ACS Appl. Mater. Inter.* 10 (51), 44518–44526. doi:10.1021/acsami.8b16962
- Chen, S., Zhao, J., Su, H., Li, H., Wang, H., Hu, Z., et al. (2021). Pd-Pt Tesseracts for the Oxygen Reduction Reaction. *J. Am. Chem. Soc.* 143 (1), 496–503. doi:10.1021/jacs.0c12282
- Di Fabio, A., Giorgi, A., Mastragostino, M., and Soavi, F. (2001). Carbon-Poly(3-methylthiophene) Hybrid Supercapacitors. *J. Electrochem. Soc.* 148 (8), A845–A850. doi:10.1149/1.1380254
- Gao, X., Wang, P., Pan, Z., Claverie, J. P., and Wang, J. (2020). Recent Progress in Two-Dimensional Layered Double Hydroxides and Their Derivatives for Supercapacitors. *ChemSusChem* 13 (6), 1226–1254. doi:10.1002/cssc.201902753
- Gong, M., Li, Y., Wang, H., Liang, Y., Wu, J. Z., Zhou, J., et al. (2013). An Advanced Ni-Fe Layered Double Hydroxide Electrocatalyst for Water Oxidation. *J. Am. Chem. Soc.* 135 (23), 8452–8455. doi:10.1021/ja4027715
- Hall, D. S., Lockwood, D. J., Bock, C., and MacDougall, B. R. (2015). Nickel Hydroxides and Related Materials: a Review of Their Structures, Synthesis and Properties. *Proc. R. Soc. A.* 471 (2174), 20140792. doi:10.1098/rspa.2014.0792
- Huang, J., Lei, T., Wei, X., Liu, X., Liu, T., Cao, D., et al. (2013). Effect of Al-Doped β -Ni(OH)₂ Nanosheets on Electrochemical Behaviors for High Performance Supercapacitor Application. *J. Power Sourc.* 232, 370–375. doi:10.1016/j.jpowsour.2013.01.081
- Huang, W., Ma, X. Y., Wang, H., Feng, R., Zhou, J., Duchesne, P. N., et al. (2017). Promoting Effect of Ni(OH)₂ on Palladium Nanocrystals Leads to Greatly Improved Operation Durability for Electrocatalytic Ethanol Oxidation in Alkaline Solution. *Adv. Mater.* 29 (37), 1703057. doi:10.1002/adma.201703057
- Hunter, B. M., Hieringer, W., Winkler, J. R., Gray, H. B., and Müller, A. M. (2016). Effect of Interlayer Anions on [NiFe]-LDH Nanosheet Water Oxidation Activity. *Energy Environ. Sci.* 9 (5), 1734–1743. doi:10.1039/c6ee00377j
- Jian, X. W., Zhu, Y. J., Li, W. H., and Zhao, T. Q. (2016). Crystal Phase, Structure Stability and Electrochemical Performance of Co/Cu/Al-Substituted Nano-Sized Alpha Nickel Hydroxide. *Appl. Phys. A.* 122 (10), 1–9. doi:10.1007/s00339-016-0443-7
- Jiang, H., Zhao, T., Li, C., and Ma, J. (2011). Hierarchical Self-Assembly of Ultrathin Nickel Hydroxide Nanoflakes for High-Performance Supercapacitors. *J. Mater. Chem.* 21 (11), 3818–3823. doi:10.1039/c0jm03830j
- Kalam, A., Al-Shihri, A. S., Al-Sehemi, A. G., Awwad, N. S., Du, G., and Ahmad, T. (2013). Effect of pH on Solvothermal Synthesis of β -Ni(OH)₂ and NiO Nano-Architectures: Surface Area Studies, Optical Properties and Adsorption Studies. *Superlattices and Microstructures* 55, 83–97. doi:10.1016/j.spmi.2012.11.024
- Kang, G., Zhu, Z., Tang, B.-H., Wu, C.-H., and Wu, R.-J. (2017). Rapid Detection of Ozone in the Parts Per Billion Range Using a Novel Ni-Al Layered Double Hydroxide. *Sensors Actuators B: Chem.* 241, 1203–1209. doi:10.1016/j.snb.2016.10.012
- Kötz, R., and Carlen, M. (2000). Principles and Applications of Electrochemical Capacitors. *Electrochimica Acta* 45 (15-16), 2483–2498. doi:10.1016/s0013-4686(00)00354-6
- Lakshmi, V., Ranjusha, R., Vineeth, S., Nair, S. V., and Balakrishnan, A. (2014). Supercapacitors Based on Microporous β -Ni(OH)₂ Nanorods. *Colloids Surf. A: Physicochemical Eng. Aspects* 457, 462–468. doi:10.1016/j.colsurfa.2014.06.016
- Li, B., Ai, M., and Xu, Z. (2010). Mesoporous β -Ni(OH)₂: Synthesis and Enhanced Electrochemical Performance. *Chem. Commun.* 46 (34), 6267–6269. doi:10.1039/c0cc00155d
- Li, C., Wei, M., Evans, D. G., and Duan, X. (2014). Layered Double Hydroxide-Based Nanomaterials as Highly Efficient Catalysts and Adsorbents. *Small* 10 (22), 4469–4486. doi:10.1002/sml.201401464
- Li, G., Zhang, X., Qiu, D., Liu, Z., Yang, C., Cockreham, C. B., et al. (2019). Tuning Ni/Al Ratio to Enhance Pseudocapacitive Charge Storage Properties of Nickel-

- Aluminum Layered Double Hydroxide. *Adv. Electron. Mater.* 5 (8), 1900215. doi:10.1002/aelm.201900215
- Li, H., Liu, S., Huang, C., Zhou, Z., Li, Y., and Fang, D. (2011). Characterization and Supercapacitor Application of coin-like β -nickel Hydroxide Nanoplates. *Electrochimica Acta* 58, 89–94. doi:10.1016/j.electacta.2011.08.120
- Li, Z. H. A. O., Liu, Z. H., and Lei, J. I. N. (2013). Preparation and Electrochemical Performance of Nano-Scale Ni(OH)₂ Doped with Zinc. *Trans. Nonferrous Met. Soc. China* 23 (4), 1033–1038. doi:10.1016/s1003-6326(13)62563-7
- Liu, H., Wang, Y., Lu, X., Hu, Y., Zhu, G., Chen, R., et al. (2017). The Effects of Al Substitution and Partial Dissolution on Ultrathin NiFeAl Ternary Layered Double Hydroxide Nanosheets for Oxygen Evolution Reaction in Alkaline Solution. *Nano Energy* 35, 350–357. doi:10.1016/j.nanoen.2017.04.011
- Liu, J., Cheng, C., Zhou, W., Li, H., and Fan, H. J. (2011). Ultrathin Nickel Hydroxidenitrate Nanoflakes Branched on Nanowire Arrays for High-Rate Pseudocapacitive Energy Storage. *Chem. Commun.* 47 (12), 3436–3438. doi:10.1039/c0cc04906a
- Liu, W., Sun, J., Zhang, X., and Wei, M. (2018). Supported Ag Catalysts on Mg-Al Oxides toward Oxidant-free Dehydrogenation Reaction of Benzyl Alcohol. *Ind. Eng. Chem. Res.* 57 (46), 15606–15612. doi:10.1021/acs.iecr.8b03987
- Luo, Z., Wang, K., Li, H., Yin, S., Guan, Q., and Wang, L. (2011). One-dimensional β -Ni(OH)₂ Nanostructures: Ionic Liquid Etching Synthesis, Formation Mechanism, and Application for Electrochemical Capacitors. *CrystEngComm* 13 (23), 7108–7113. doi:10.1039/c1ce05936j
- Mao, Y., Zhou, B., and Peng, S. (2020). Simple Deposition of Mixed α , β -nickel Hydroxide Thin Film onto Nickel Foam as High-Performance Supercapacitor Electrode Material. *J. Mater. Sci. Mater. Electron.* 31, 9457–9467. doi:10.1007/s10854-020-03485-6
- Mishra, G., Dash, B., and Pandey, S. (2018). Layered Double Hydroxides: A Brief Review from Fundamentals to Application as Evolving Biomaterials. *Appl. Clay Sci.* 153, 172–186. doi:10.1016/j.clay.2017.12.021
- Neiva, E. G. C., Oliveira, M. M., Bergamini, M. F., Marcolino, L. H., and Zarbin, A. J. G. (2016). One Material, Multiple Functions: graphene/Ni(OH)₂ Thin Films Applied in Batteries, Electrochromism and Sensors. *Sci. Rep.* 6 (1), 1–14. doi:10.1038/srep33806
- Oliva, P., Leonardi, J., Laurent, J. F., Delmas, C., Braconnier, J. J., Figlarz, M., et al. (1982). Review of the Structure and the Electrochemistry of Nickel Hydroxides and Oxy-Hydroxides. *J. Power Sourc.* 8 (2), 229–255. doi:10.1016/0378-7753(82)80057-8
- Park, J. H., Kim, S., Park, O. O., and Ko, J. M. (2006). Improved Asymmetric Electrochemical Capacitor Using Zn-Co Co-doped Ni(OH)₂ Positive Electrode Material. *Appl. Phys. A.* 82 (4), 593–597. doi:10.1007/s00339-005-3400-4
- Šekularac, G., Košević, M., Dekanski, A., Djokić, V., Panjan, M., and Panić, V. (2017). High Energy/power Supercapacitor Performances of Intrinsically Ordered Ruthenium Oxide Prepared through Fast Hydrothermal Synthesis. *ChemElectroChem* 4 (10), 2535–2541. doi:10.1002/celec.201700609
- Shao, G., Yao, Y., Zhang, S., and He, P. (2009). Supercapacitor Characteristic of La-Doped Ni(OH)₂ Prepared by Electrode-Position. *Rare Met.* 28 (2), 132–136. doi:10.1007/s12598-009-0026-2
- Shao, M., Ning, F., Zhao, Y., Zhao, J., Wei, M., Evans, D. G., et al. (2012). Core-shell Layered Double Hydroxide Microspheres with Tunable interior Architecture for Supercapacitors. *Chem. Mater.* 24 (6), 1192–1197. doi:10.1021/cm203831p
- Shen, C., Li, R., Yan, L., Shi, Y., Guo, H., Zhang, J., et al. (2018). Rational Design of Activated Carbon Nitride Materials for Symmetric Supercapacitor Applications. *Appl. Surf. Sci.* 455, 841–848. doi:10.1016/j.apsusc.2018.06.065
- Simon, P., and Gogotsi, Y. (2008). Materials for Electrochemical Capacitors. *Nat. Mater.* 7, 845–854. doi:10.1038/nmat2297
- Tang, Y., Liu, Y., Yu, S., Zhao, Y., Mu, S., and Gao, F. (2014). Hydrothermal Synthesis of a Flower-like Nano-Nickel Hydroxide for High Performance Supercapacitors. *Electrochimica Acta* 123, 158–166. doi:10.1016/j.electacta.2013.12.187
- Tian, Y., Zhou, X., Huang, L., and Liu, M. (2013). A Facile Gas-Liquid Co-deposition Method to Prepare Nanostructured Nickel Hydroxide for Electrochemical Capacitors. *J. Inorg. Organomet. Polym.* 23 (6), 1425–1430. doi:10.1007/s10904-013-9945-3
- Tizfahm, J., Safibonab, B., Aghazadeh, M., Majdabadi, A., Sabour, B., and Dalvand, S. (2014). Supercapacitive Behavior of β -Ni(OH)₂ Nanospheres Prepared by a Facile Electrochemical Method. *Colloids Surf. A: Physicochemical Eng. Aspects* 443, 544–551. doi:10.1016/j.colsurfa.2013.12.024
- Vidotti, M., van Greco, C., Ponzio, E. A., and Córdoba de Torresi, S. I. (2006). Sonochemically Synthesized Ni(OH)₂ and Co(OH)₂ Nanoparticles and Their Application in Electrochromic Electrodes. *Electrochemistry Commun.* 8 (4), 554–560. doi:10.1016/j.elecom.2006.01.024
- Wang, H., Casalongue, H. S., Liang, Y., and Dai, H. (2010). Ni(OH)₂ Nanoplates Grown on Graphene as Advanced Electrochemical Pseudocapacitor Materials. *J. Am. Chem. Soc.* 132 (21), 7472–7477. doi:10.1021/ja102267j
- Wang, L., Li, J., Wang, M., Liu, Y., and Cui, H. (2019). In Situ synthesis of Two-dimensional Co²⁺-Doped β -Ni(OH)₂ Using Nickel Complex as Template for Application in Supercapacitors. *J. Sol-gel Sci. Technol.* 89 (2), 492–499. doi:10.1007/s10971-018-4880-y
- Wang, X., Wu, F., Fan, J., Tian, A., Cheng, Y., and Yang, S. (2021). High Specific Surface Area NiTiAl Layered Double Hydroxide Derived via Alkali Etching for High Performance Supercapacitor Electrode. *J. Alloys Comp.* 888, 161502. doi:10.1016/j.jallcom.2021.161502
- Wang, Y.-M., Zhao, D.-D., Zhao, Y.-Q., Xu, C.-L., and Li, H.-L. (2012). Effect of Electrodeposition Temperature on the Electrochemical Performance of a Ni(OH)₂ electrode. *RSC Adv.* 2 (3), 1074–1082. doi:10.1039/c1ra00613d
- Wang, Y., Gai, S., Li, C., He, F., Zhang, M., Yan, Y., et al. (2013). Controlled Synthesis and Enhanced Supercapacitor Performance of Uniform Pompon-like β -Ni(OH)₂ Hollow Microspheres. *Electrochimica Acta* 90, 673–681. doi:10.1016/j.electacta.2012.11.136
- Wang, Y., Hao, X., Wang, G., and Jin, Z. (2021). Rational Design of a Core-Shell Shaped Flowerlike Mn_{0.05}Cd_{0.95}S@NiAl-LDH Structure for Efficient Hydrogen Evolution. *Catal. Lett.* 151 (3), 634–647. doi:10.1007/s10562-020-03346-1
- Wang, Z., Xu, S.-M., Xu, Y., Tan, L., Wang, X., Zhao, Y., et al. (2019). Single Ru Atoms with Precise Coordination on a Monolayer Layered Double Hydroxide for Efficient Electrooxidation Catalysis. *Chem. Sci.* 10 (2), 378–384. doi:10.1039/c8sc04480e
- Wu, X., Ci, C., Du, Y., Liu, X., Li, X., and Xie, X. (2018). Facile Synthesis of NiAl-LDHs with Tunable Establishment of Acid-Base Activity Sites. *Mater. Chem. Phys.* 211, 72–78. doi:10.1016/j.matchemphys.2018.02.015
- Xiao-yan, G., and Jian-Cheng, D. (2007). Preparation and Electrochemical Performance of Nano-Scale Nickel Hydroxide with Different Shapes. *Mater. Lett.* 61 (3), 621–625. doi:10.1016/j.matlet.2006.05.026
- Xu, M., and Wei, M. (2018). Layered Double Hydroxide-Based Catalysts: Recent Advances in Preparation, Structure, and Applications. *Adv. Funct. Mater.* 28 (47), 1802943. doi:10.1002/adfm.201802943
- Yan, H., Wang, J., Li, S., Yang, W., Gao, Z., Liu, Q., et al. (2013). L-Lysine Assisted Synthesis of β -Ni(OH)₂ Hierarchical Hollow Microspheres and Their Enhanced Electrochemical Capacitance Performance. *Electrochimica Acta* 87, 880–888. doi:10.1016/j.electacta.2012.08.090
- Ye, X., Jiang, Z., Li, L., and Xie, Z.-H. (2018). In-situ Growth of NiAl-Layered Double Hydroxide on AZ31 Mg alloy towards Enhanced Corrosion protection. *Nanomaterials* 8 (6), 411. doi:10.3390/nano8060411
- Yin, H., and Tang, Z. (2016). Ultrathin Two-Dimensional Layered Metal Hydroxides: an Emerging Platform for Advanced Catalysis, Energy Conversion and Storage. *Chem. Soc. Rev.* 45 (18), 4873–4891. doi:10.1039/c6cs00343e
- Yu, D., Qian, Q., Wei, L., Jiang, W., Goh, K., Wei, J., et al. (2015). Emergence of Fiber Supercapacitors. *Chem. Soc. Rev.* 44 (3), 647–662. doi:10.1039/c4cs00286e
- Yu, J., Wang, Q., O'Hare, D., and Sun, L. (2017). Preparation of Two Dimensional Layered Double Hydroxide Nanosheets and Their Applications. *Chem. Soc. Rev.* 46 (19), 5950–5974. doi:10.1039/c7cs00318h
- Zang, J., Bao, S.-J., Li, C. M., Bian, H., Cui, X., Bao, Q., et al. (2008). Well-Aligned Cone-Shaped Nanostructure of Polypyrrole/RuO₂ and its Electrochemical Supercapacitor. *J. Phys. Chem. C* 112 (38), 14843–14847. doi:10.1021/jp8049558
- Zhai, Z., Liu, Q., Zhu, Y., Cao, J., and Shi, S. (2019). Synthesis of Ni(OH)₂/graphene Composite with Enhanced Electrochemical Property by Stirring Solvothermal Method. *J. Alloys Comp.* 775, 1316–1323. doi:10.1016/j.jallcom.2018.10.262

- Zhang, S., Fan, Q., Liu, Y., Xi, S., Liu, X., Wu, Z., et al. (2020). Dehydration-Triggered Ionic Channel Engineering in Potassium Niobate for Li/K-Ion Storage. *Adv. Mater.* 32 (22), 2000380. doi:10.1002/adma.202000380
- Zhang, S., Liu, Y., Fan, Q., Zhang, C., Zhou, T., Kalantar-Zadeh, K., et al. (2021). Liquid Metal Batteries for Future Energy Storage. *Energ. Environ. Sci.* doi:10.1039/D1EE00531F
- Zhang, W., Xu, C., Ma, C., Li, G., Wang, Y., Zhang, K., et al. (2017). Nitrogen-Superdoped 3D Graphene Networks for High-Performance Supercapacitors. *Adv. Mater.* 29 (36), 1701677. doi:10.1002/adma.201701677
- Zhao, M., Zhao, Q., Li, B., Xue, H., Pang, H., and Chen, C. (2017). Recent Progress in Layered Double Hydroxide Based Materials for Electrochemical Capacitors: Design, Synthesis and Performance. *Nanoscale* 9 (40), 15206–15225. doi:10.1039/c7nr04752e
- Zhou, J., Liu, Y., Zhang, S., Zhou, T., and Guo, Z. (2020). Metal Chalcogenides for Potassium Storage. *InfoMat* 2 (3), 437–465. doi:10.1002/inf2.12101
- Zhou, X., Cao, D., Huang, J., Ye, K., Yang, S., Liu, T., et al. (2014). Capacitance Performance of Nanostructured β -Ni(OH)₂ with Different Morphologies Grown on Nickel Foam. *J. Electroanalytical Chem.* 720-721, 115–120. doi:10.1016/j.jelechem.2014.03.020

Conflict of Interest: The authors declare that the research was conducted in the absence of any commercial or financial relationships that could be construed as a potential conflict of interest.

Publisher's Note: All claims expressed in this article are solely those of the authors and do not necessarily represent those of their affiliated organizations, or those of the publisher, the editors, and the reviewers. Any product that may be evaluated in this article, or claim that may be made by its manufacturer, is not guaranteed or endorsed by the publisher.

Copyright © 2022 Chen, Yang, Tian, Wang, Zhao, Lei and Zhang. This is an open-access article distributed under the terms of the Creative Commons Attribution License (CC BY). The use, distribution or reproduction in other forums is permitted, provided the original author(s) and the copyright owner(s) are credited and that the original publication in this journal is cited, in accordance with accepted academic practice. No use, distribution or reproduction is permitted which does not comply with these terms.